Spin-Axis Stabilization of a Rigid Body about an Arbitrary Direction using Two Reaction Wheels

Kyunam Kim, *Graduate Student Member, IEEE*, and Alice M. Agogino, *Senior Member, IEEE*

***Abstract*— The purpose of attitude stabilization is to stabilize a body about an equilibrium point, usually requiring at least three independent actuations. In practice, however, a control law for an underactuated system with two actuators becomes crucial when one of the three actuators fails during operation, or when the control objective is to stabilize the spin axis of the body about an arbitrary direction, possibly with a nonzero spinning velocity. In this work, we develop a feedback control law that globally and asymptotically achieves spin-axis stabilization of a rigid body about an arbitrary axis using only two reaction wheels. For this, a modified version of (z, w)-parameterization is presented for the purpose of describing attitude kinematics of a rigid body. We then introduce dynamics of the body with two reaction wheels and use a feedback linearization technique to develop a control law with the goal of achieving spin-axis stabilization of the body. We show that the developed control law is globally and asymptotically stable by using Lyapunov's direct method in conjunction with LaSalle's invariance principle. This controller is implemented in simulation, and results are presented that show its stabilizing behavior. While the control law presented here is suitable for general applications, we primarily focus on its application to the thrust direction regulation of tensegrity hoppers.**

I. Introduction

Attitude stabilization of a rigid body is, in most cases, done by using gas jet thrusters or reaction wheels. If three independent torques can be supplied by either mechanism, the system is controllable and the body can be stabilized about an equilibrium [1]. Previous research has shown that, in the case of gas jet thrusters, the body can still be stabilized about an equilibrium even when less than three independent torques are supplied, under certain conditions [1], [2]. While there exists no smooth state feedback law achieving this with only two gas jet actuators [3], a time-varying continuous feedback can locally asymptotically and exponentially stabilize the attitude of the body [4].

In the case of reaction wheels, the system with three wheels is controllable if three independent torques are supplied with a certain minimum torque level [1]. When the angular momentum of a body is zero, a discontinuous state feedback controller can be developed for the attitude stabilization of the body [5]. Recently, controllability of an underactuated satellite with two reaction wheels is analyzed and control laws are developed for the satellite's attitude stabilization for different system configurations [6], [7].

Despite the challenges of the underactuated reaction wheel systems, they are quite useful in practice due to the simplicity in their system architecture. Furthermore, they can effectively stabilize partial states of the system [2], and spin-axis stabilization using only two reaction wheels has been an important problem in this regard [8].

The goal of this work is to derive a feedback control law that stabilizes a revolute motion of a rigid body about an arbitrary direction using two reaction wheels attached to it. Specifically, we aim to develop the control law that achieves two goals: 1) the spin axis of the body is oriented towards an arbitrary target direction, and 2) the body rotates about the spin axis only, if its angular momentum is not zero.

A similar problem was discussed in [9], where several globally asymptotically stable and globally exponentially stable control laws are developed for the purpose of spin-axis stabilization of a symmetric spacecraft using two gas jet actuators. A globally asymptotically stable control law that achieves spin-axis stabilization of a spacecraft using two reaction wheels is also presented in [8]. In both works, the final direction of the spin axis is aligned with a specified inertial axis when stabilized.

In many practical applications, however, it is desirable to orient the spin axis of the primary body towards an aribitrary axis rather than an inertial axis. Consider a spacecraft or a planetary rover that utilizes an on-board thruster system as its source of mobility and assume that the thruster nozzle axis is in the direction of the spin axis of the system. During its operation, the spacecraft or the rover is occasionally required to change the orientation of the thruster nozzle such that the nozzle axis is aligned with the desired thrust direction. In such cases, however, it is unlikely that the desired thrust direction is parallel to an inertial axis.

An example case of this would be the problem of reorienting a thruster system used for hopping of tensegrity robots. Tensegrity robots are built from tensegrity structures that are composed of axially loaded compression elements suspended in a network of tensional elements [10]. The robots are inherently lightweight and naturally compliant, and recently they have been envisioned for planetary exploration rovers [11], [12], [13], [14], [15], [16], [17]. The authors have proposed to use cold gas thrusters to enable their hopping motions for traveling long distances and showed that the regulation of thrust direction is necessary in order to reduce wasting propellant used in moving towards undesirable directions [15]. Furthermore, the desired thrust direction may change in between hops and in such cases the control needs to reorient the nozzle axis to match the new target direction. Hence the need for a more generalized control law arises; the law that can stabilize the nozzle axis of the thruster system towards

Kyunam Kim and Alice M. Agogino are with the Department of Mechanical Engineering, University of California at Berkeley, Berkeley, CA 94720 USA. {knkim, agogino}@berkeley.edu

an arbitrary direction. In particular, use of reaction wheels is preferrable than gas jet thrusters for the thrust regulation of hopping tensegrity robots because it allows the robots to spend propellant towards hopping only and thus increases their maximum travel distance.

To this end, we improve upon the approach taken in [8], [9] by modifying the kinematics description of a body, and then creating a controller based on this description. In Sect. II, we introduce a modified (z, w)-parameterization [18] as a way of describing the rotational kinematics of a body. We then introduce dynamics of a rigid body with two reaction wheels attached along the body's principal axes in Sect. III. We use a feedback linearization technique in Sect. IV to develop the desired control law and prove its stability via Lyapunov's direct method in conjunction with LaSalle's invariance principle. We also simulate the control on a thruster system of hopping tensegrity robots and show the controller's stabilizing behavior. Lastly, conclusion is provided in Sect. V.

II. Attitude Kinematics

In this section, we derive a set of kinematic equations describing the attitude of a rigid body, which will later be used for controller design in Sect. IV. The derivation closely follows [18] and is based on (z, w)-parameterization therein. However, we modify it to include the information of the arbitrary target direction and present a new formulation extending the prior work. This modification is necessary in order to develop the controller that stabilizes the spin axis of the body about an arbitrary direction.

A. Parameterization of Rotations

Let the two sets of orthonormal right-handed basis vectors for the inertial and body-fixed reference frames be $\{\mathbf{E}_1, \mathbf{E}_2, \mathbf{E}_3\}$ and $\{\mathbf{e}_1, \mathbf{e}_2, \mathbf{e}_3\}$, respectively. Then, there exists a rotation matrix $\mathbf{R} \in SO(3)$ that describes the relative orientation of the two frames. Using matrix notation, this relationship can be written as

$$\begin{bmatrix}\mathbf{e}_1\\ \mathbf{e}_2\\ \mathbf{e}_3\end{bmatrix} = \mathbf{R}\begin{bmatrix}\mathbf{E}_1\\ \mathbf{E}_2\\ \mathbf{E}_3\end{bmatrix}. \tag{1}$$

We then decompose the matrix $\mathbf{R}$ into three sub-rotations,

$$\mathbf{R} = \mathbf{R}_3(z)\mathbf{R}_2(w)\mathbf{R}_1, \tag{2}$$

where $\mathbf{R}_1, \mathbf{R}_2(w), \mathbf{R}_3(z) \in SO(3)$. Note that the two rotations $\mathbf{R}_2(w)$ and $\mathbf{R}_3(z)$ are parameterized by w and z, which are functions of time. $\mathbf{R}_1$ is not parameterized because we assume this matrix is constant in this work, as will be discussed later.

Furthermore, we define two additional sets of orthonormal right-handed basis vectors $\{\mathbf{t}_1, \mathbf{t}_2, \mathbf{t}_3\}$ and $\{\mathbf{e}'_1, \mathbf{e}'_2, \mathbf{e}'_3\}$ to describe intermediate reference frames during the rotation $\mathbf{R}$ (Fig. 1). The relationships between the rotation matrices and the basis vectors are given as

$$\begin{bmatrix}\mathbf{t}_1\\ \mathbf{t}_2\\ \mathbf{t}_3\end{bmatrix} = \mathbf{R}_1\begin{bmatrix}\mathbf{E}_1\\ \mathbf{E}_2\\ \mathbf{E}_3\end{bmatrix}, \tag{3}$$

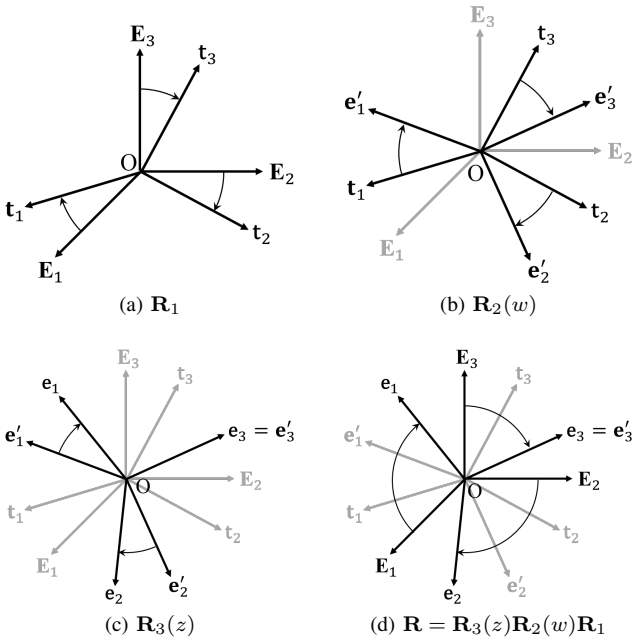

(a) $\mathbf{R}_1$ (b) $\mathbf{R}_2(w)$ (c) $\mathbf{R}_3(z)$ (d) $\mathbf{R} = \mathbf{R}_3(z)\mathbf{R}_2(w)\mathbf{R}_1$

Fig. 1. Rotations and basis vectors used to describe attitude kinematics of a rigid body. The rotation $\mathbf{R}$ between the inertial frame and body-fixed frame consists of three sub-rotations. (a) The first rotation rotates $\{\mathbf{E}_1, \mathbf{E}_2, \mathbf{E}_3\}$ to $\{\mathbf{t}_1, \mathbf{t}_2, \mathbf{t}_3\}$. $\mathbf{t}_3$ is the target direction about which the spin axis of the body will be stabilized. (b) The second rotation rotates $\{\mathbf{t}_1, \mathbf{t}_2, \mathbf{t}_3\}$ to $\{\mathbf{e}'_1, \mathbf{e}'_2, \mathbf{e}'_3\}$. (c) The third rotation is about the axis $\mathbf{e}'_3 = \mathbf{e}_3$, and it rotates $\{\mathbf{e}'_1, \mathbf{e}'_2, \mathbf{e}'_3\}$ to $\{\mathbf{e}_1, \mathbf{e}_2, \mathbf{e}_3\}$. (d) The overall rotation $\mathbf{R}$ is a combination of $\mathbf{R}_1$, $\mathbf{R}_2(w)$ and $\mathbf{R}_3(z)$.

$$\begin{bmatrix}\mathbf{e}'_1\\ \mathbf{e}'_2\\ \mathbf{e}'_3\end{bmatrix} = \mathbf{R}_2(w)\begin{bmatrix}\mathbf{t}_1\\ \mathbf{t}_2\\ \mathbf{t}_3\end{bmatrix}, \tag{4}$$

$$\begin{bmatrix}\mathbf{e}_1\\ \mathbf{e}_2\\ \mathbf{e}_3\end{bmatrix} = \mathbf{R}_3(z)\begin{bmatrix}\mathbf{e}'_1\\ \mathbf{e}'_2\\ \mathbf{e}'_3\end{bmatrix}. \tag{5}$$

We let $\mathbf{t}_3$ be the direction about which the spin axis of the body will be stabilized. Letting $\mathbf{e}_3$ represent the current spin axis of the rigid body, the control objective will then be to align $\mathbf{t}_3$ and $\mathbf{e}_3$. Moreover, we assume the target direction $\mathbf{t}_3$ is known a priori and time independent in this work. Then, the first rotation $\mathbf{R}_1$ is not an arbitrary rotation, but rather it is a constant rotation that rotates the third inertial axis $\mathbf{E}_3$ to $\mathbf{t}_3$. As a result, $\mathbf{R}_1$ is a constant matrix. From [18], it is known that such a rotation has the form of

$$\mathbf{R}_1 = \begin{bmatrix} k_3 + \frac{k_2^2}{1+k_3} & -\frac{k_1 k_2}{1+k_3} & k_1 \\ -\frac{k_1 k_2}{1+k_3} & k_3 + \frac{k_1^2}{1+k_3} & k_2 \\ -k_1 & -k_2 & k_3 \end{bmatrix}, \tag{6}$$

with the constants k_1, k_2 and k_3 satisfying the constraint

$$k_1^2 + k_2^2 + k_3^2 = 1. \tag{7}$$

Next, the second rotation $\mathbf{R}_2(w)$ rotates $\mathbf{t}_3$ to $\mathbf{e}'_3$, which is identical to $\mathbf{e}_3$ if we let $\mathbf{e}'_3$ to be the rotation axis of the third rotation $\mathbf{R}_3(z)$. As a result, the second rotation $\mathbf{R}_2(w)$

rotates $\mathbf{t}_3$ to $\mathbf{e}_3$. $\mathbf{R}_2(w)$ has a form similar to $\mathbf{R}_1$ and can be written as

$$\mathbf{R}_2(w) = \begin{bmatrix} c + \frac{b^2}{1+c} & -\frac{ab}{1+c} & a \\ -\frac{ab}{1+c} & c + \frac{a^2}{1+c} & b \\ -a & -b & c \end{bmatrix}, \tag{8}$$

with the parameters a, b and c satisfying the constraint

$$a^2 + b^2 + c^2 = 1. \tag{9}$$

Unlike k_1, k_2 and k_3, notice that a, b and c are functions of time because their values change as the body rotates. By using a stereographic projection, the constraint (9) can be incorporated into (8) [18]. If we define a complex variable $w = w_1 + iw_2$ as

$$w = \frac{b - ia}{1 + c}, \tag{10}$$

$\mathbf{R}_2(w)$ can be re-written as

$$\mathbf{R}_2(w) = \frac{1}{1 + w_1^2 + w_2^2} \times \begin{bmatrix} 1 + w_1^2 - w_2^2 & 2w_1 w_2 & -2w_2 \\ 2w_1 w_2 & 1 - w_1^2 + w_2^2 & 2w_1 \\ 2w_2 & -2w_1 & 1 - w_1^2 - w_2^2 \end{bmatrix}. \tag{11}$$

The final rotation $\mathbf{R}_3(z)$ is the rotation about $\mathbf{e}_3 = \mathbf{e}_3'$ and is given by

$$\mathbf{R}_3(z) = \begin{bmatrix} \cos(z) & \sin(z) & 0 \\ -\sin(z) & \cos(z) & 0 \\ 0 & 0 & 1 \end{bmatrix}. \tag{12}$$

B. Kinematic Equations

By substituting (6), (8) and (12) into (2), we can find the expression of $\mathbf{R}$ in terms of k_1, k_2, k_3, a, b, c and z. Although we will not write the full expression of $\mathbf{R}$ here, we do note that the third row of $\mathbf{R}$ is independent of the parameter z. Consider the inverse rotation of $\mathbf{R}$ and define

$$\widetilde{\mathbf{R}} = \mathbf{R}^{-1} = \mathbf{R}^{\mathrm{T}}. \tag{13}$$

If we denote $\mathbf{R}_{(i,*)}$ as the i-th row of $\mathbf{R}$, and $\widetilde{\mathbf{R}}_{(*,j)}$ as the j-th column of $\widetilde{\mathbf{R}}$, we have

$$\widetilde{\mathbf{R}}_{(*,3)} = [\mathbf{R}_{(3,*)}]^{\mathrm{T}} = \mathbf{A} \begin{bmatrix} a \\ b \\ c \end{bmatrix}, \tag{14}$$

where we introduced a constant matrix $\mathbf{A}$ defined as

$$\mathbf{A} = \begin{bmatrix} -(k_3 + \frac{k_2^2}{1+k_3}) & \frac{k_1 k_2}{1+k_3} & -k_1 \\ \frac{k_1 k_2}{1+k_3} & -(k_3 + \frac{k_1^2}{1+k_3}) & -k_2 \\ -k_1 & -k_2 & k_3 \end{bmatrix}. \tag{15}$$

Notice that $\mathbf{A}$ is an involutory matrix and $\mathbf{A}^{-1} = \mathbf{A}$.

Furthermore, let us introduce two angular velocities $\boldsymbol{\omega}$ and $\widetilde{\boldsymbol{\omega}}$. $\boldsymbol{\omega}$ is the angular velocity vector of the body frame $\{\mathbf{e}_1, \mathbf{e}_2, \mathbf{e}_3\}$ with respect to the inertial frame $\{\mathbf{E}_1, \mathbf{E}_2, \mathbf{E}_3\}$, whereas $\widetilde{\boldsymbol{\omega}}$ is the angular velocity vector of the inertial frame $\{\mathbf{E}_1, \mathbf{E}_2, \mathbf{E}_3\}$ with respect to the body frame $\{\mathbf{e}_1, \mathbf{e}_2, \mathbf{e}_3\}$. We write $\boldsymbol{\omega}$ and $\widetilde{\boldsymbol{\omega}}$ as

$$\begin{aligned} \boldsymbol{\omega} &= \omega_1 \mathbf{e}_1 + \omega_2 \mathbf{e}_2 + \omega_3 \mathbf{e}_3 \\ &= \omega_1^E \mathbf{E}_1 + \omega_2^E \mathbf{E}_2 + \omega_3^E \mathbf{E}_3, \end{aligned} \tag{16}$$

and

$$\widetilde{\boldsymbol{\omega}} = \widetilde{\omega}_1 \mathbf{E}_1 + \widetilde{\omega}_2 \mathbf{E}_2 + \widetilde{\omega}_3 \mathbf{E}_3. \tag{17}$$

By definition, $\boldsymbol{\omega}$ and $\widetilde{\boldsymbol{\omega}}$ has the relationship

$$\widetilde{\boldsymbol{\omega}} = -\boldsymbol{\omega}, \tag{18}$$

in the inertial frame. In terms of components, this can be re-written as

$$\begin{bmatrix} \widetilde{\omega}_1 \\ \widetilde{\omega}_2 \\ \widetilde{\omega}_3 \end{bmatrix} = - \begin{bmatrix} \omega_1^E \\ \omega_2^E \\ \omega_3^E \end{bmatrix} = -\mathbf{R}^{\mathrm{T}} \begin{bmatrix} \omega_1 \\ \omega_2 \\ \omega_3 \end{bmatrix}. \tag{19}$$

With the help of skew-symmetric matrices

$$\mathbf{S}(\boldsymbol{\omega}) = \begin{bmatrix} 0 & \omega_3 & -\omega_2 \\ -\omega_3 & 0 & \omega_1 \\ \omega_2 & -\omega_1 & 0 \end{bmatrix}, \tag{20}$$

and

$$\mathbf{S}(\widetilde{\boldsymbol{\omega}}) = \begin{bmatrix} 0 & \widetilde{\omega}_3 & -\widetilde{\omega}_2 \\ -\widetilde{\omega}_3 & 0 & \widetilde{\omega}_1 \\ \widetilde{\omega}_2 & -\widetilde{\omega}_1 & 0 \end{bmatrix}, \tag{21}$$

the time derivatives of the rotation matrices $\mathbf{R}$ and $\widetilde{\mathbf{R}}$ are related to the angular velocities $\boldsymbol{\omega}$ and $\widetilde{\boldsymbol{\omega}}$ as

$$\dot{\mathbf{R}} = \mathbf{S}(\boldsymbol{\omega})\mathbf{R}, \tag{22}$$

and

$$\dot{\widetilde{\mathbf{R}}} = \mathbf{S}(\widetilde{\boldsymbol{\omega}})\widetilde{\mathbf{R}}. \tag{23}$$

Moreover, if we consider only the third column of $\dot{\widetilde{\mathbf{R}}}$ in (23),

$$\dot{\widetilde{\mathbf{R}}}_{(*,3)} = \mathbf{S}(\widetilde{\boldsymbol{\omega}})\widetilde{\mathbf{R}}_{(*,3)}, \tag{24}$$

and by substituting (14) into (24), we obtain

$$\begin{bmatrix} \dot{a} \\ \dot{b} \\ \dot{c} \end{bmatrix} = \mathbf{A}\mathbf{S}(\widetilde{\boldsymbol{\omega}})\mathbf{A} \begin{bmatrix} a \\ b \\ c \end{bmatrix}. \tag{25}$$

After some algebra, it turns out that the matrix $\mathbf{A}\mathbf{S}(\widetilde{\boldsymbol{\omega}})\mathbf{A}$ is also skew-symmetric and has the form of

$$\mathbf{A}\mathbf{S}(\widetilde{\boldsymbol{\omega}})\mathbf{A} = \begin{bmatrix} 0 & \widetilde{\eta}_3 & -\widetilde{\eta}_2 \\ -\widetilde{\eta}_3 & 0 & \widetilde{\eta}_1 \\ \widetilde{\eta}_2 & -\widetilde{\eta}_1 & 0 \end{bmatrix} = \mathbf{S}(\widetilde{\boldsymbol{\eta}}), \tag{26}$$

where

$$\widetilde{\boldsymbol{\eta}} = \begin{bmatrix} \widetilde{\eta}_1 \\ \widetilde{\eta}_2 \\ \widetilde{\eta}_3 \end{bmatrix} = \mathbf{A} \begin{bmatrix} \widetilde{\omega}_1 \\ \widetilde{\omega}_2 \\ \widetilde{\omega}_3 \end{bmatrix} = -\mathbf{A}\mathbf{R}^{\mathrm{T}} \begin{bmatrix} \omega_1 \\ \omega_2 \\ \omega_3 \end{bmatrix}. \tag{27}$$

We used (19) to obtain the last equality in (27).

In [18], it was shown that the system of differential equations in (25) can be transformed into two scalar differential

equations by using the complex projection variable w as defined in (10):

$$\dot{w}_1 = w_2\widetilde{\eta}_3 + w_1 w_2 \widetilde{\eta}_2 + \frac{\widetilde{\eta}_1}{2}(1 + w_1^2 - w_2^2), \tag{28}$$

$$\dot{w}_2 = -w_1\widetilde{\eta}_3 + w_1 w_2 \widetilde{\eta}_1 + \frac{\widetilde{\eta}_2}{2}(1 - w_1^2 + w_2^2). \tag{29}$$

By substituting (27) into (28) and (29), the above differential equations can be re-written as

$$\dot{w}_1 = \frac{1}{2}(1 + w_1^2 + w_2^2)(\omega_1 \cos(z) - \omega_2 \sin(z)), \tag{30}$$

$$\dot{w}_2 = \frac{1}{2}(1 + w_1^2 + w_2^2)(\omega_1 \sin(z) + \omega_2 \cos(z)). \tag{31}$$

The differential equation for the z-rotation is obtained by equating the first elements of both sides of (22) and using (30) and (31). That is,

$$\dot{z} = \omega_3 + (\omega_2 w_1 - \omega_1 w_2)\cos(z) + (\omega_1 w_1 + \omega_2 w_2)\sin(z). \tag{32}$$

The new kinematic equations (30)–(32) describe the attitude of the body with respect to the target orientation.

C. Remarks

In its original form, the (z, w)-parameterization decomposes a rotation between the inertial and body-fixed reference frames into two successive rotations, namely, z- and w-rotations, and decouples the kinematic equation of w-rotation from that of z-rotation. In this work, we have modified the parameterization to explicitly include the target direction $\mathbf{t}_3$ by adding a new rotation $\mathbf{R}_1$. Because of this added rotation, the decoupling of w- and z-rotations is removed, but the resultant kinematic equations are yet simple enough to develop the desired spin-axis stabilization control law.

When we decompose $\mathbf{R}$, we take w-rotation before z-rotation, which is the reversed order of what is presented in [18]. This order of rotations is chosen because it results in the third row of $\mathbf{R}$, or the third column of $\widetilde{\mathbf{R}}$, being independent of z as provided in (14), and allows us to derive the differential kinematic equations (25), (30) and (31).

The representation has a singularity when $a = b = 0$ and $c = -1$, originating from the stereographic projection (10). In this case, $\mathbf{e}_3 = -\mathbf{t}_3$ and the spin axis of the body is pointing exactly the opposite of the target direction. This singularity case may be overcome by first attempting to stabilize $\mathbf{e}_3$ about some direction $\mathbf{t}_3' \neq \mathbf{t}_3$. Once this is done, the control can then stabilize $\mathbf{e}_3 = \mathbf{t}_3'$ to $\mathbf{t}_3$. We provide a simulation of this singular case in Sect. IV-C.

III. Dynamics of Rigid Body with Two Reaction Wheels

Let the basis vectors $\{\mathbf{e}_1, \mathbf{e}_2, \mathbf{e}_3\}$ be chosen to be coincident with the principal axes of the primary rigid body. We assume that there are two identical axis-symmetric reaction wheels attached to this rigid body, and their rotation axes are aligned with $\mathbf{e}_1$ and $\mathbf{e}_2$. It is well-known that the dynamics of such a system are given by (see, for example, [8], [19])

$$(I_1 - J_a)\dot{\omega}_1 = (I_2 - I_3)\omega_2\omega_3 + h_2\omega_3 - u_1, \tag{33}$$

$$(I_2 - J_a)\dot{\omega}_2 = (I_3 - I_1)\omega_3\omega_1 - h_1\omega_3 - u_2, \tag{34}$$

$$I_3\dot{\omega}_3 = (I_1 - I_2)\omega_1\omega_2 - h_2\omega_1 + h_1\omega_2, \tag{35}$$

$$\dot{h}_1 = -J_a\dot{\omega}_1 + u_1, \tag{36}$$

$$\dot{h}_2 = -J_a\dot{\omega}_2 + u_2. \tag{37}$$

In (33)–(37), I_i is the moment of inertia of the system, including the rigid body and the reaction wheels, along $\mathbf{e}_i$ direction. Specifically, if I_i^b represents the moment of inertia of the rigid body in $\mathbf{e}_i$ direction, and J_a and J_t represent the axial and transverse moments of inertia of the wheels, respectively, then

$$I_{1,2} = I_{1,2}^b + J_a + J_t, \qquad I_3 = I_3^b + 2J_t. \tag{38}$$

Notice that $I_i - J_a > 0$ for $i = 1, 2$ in (33) and (34). ω_j is the component of the angular velocity of the rigid body in $\mathbf{e}_j$ direction, observed in the body reference frame, as given in (16). If we let Ω_k $(k = 1, 2)$ represent the relative angular speed of the k-th wheel with respect to the rigid body, then $h_k = J_a\Omega_k$ is the relative angular momentum of the k-th wheel. Finally, u_l $(l = 1, 2)$ is the input control torque to the wheel l. As a reaction to this input, $-u_l$ is also applied to the primary body.

IV. Controls for Spin-Axis Stabilization

A. Control Objective and Equilibrium

We want the spin axis of the primary body $\mathbf{e}_3$ to be aligned with the known target direction $\mathbf{t}_3$. From (4) and (5), we find that this goal is achieved when $\mathbf{R}_2(w) = \mathbf{I}$, where $\mathbf{I}$ is an identity matrix. As a consequence, we want to converge to the state where $a^* = b^* = 0$ and $c^* = 1$, or equivalently, $w_1^* = w_2^* = 0$, where the superscript * is used to denote the converged values. At convergence, $\dot{w}_1^* = \dot{w}_2^* = 0$, which implies that $\omega_1^* = \omega_2^* = 0$, and thus $\dot{\omega}_1^* = \dot{\omega}_2^* = 0$, as can be seen from (30) and (31). Additionally, (32) and (35) say that $\dot{z}^* = \omega_3^*$ and $\dot{\omega}_3^* = 0$, that is, the primary body rotates about $\mathbf{e}_3 = \mathbf{t}_3$ at a constant angular speed of ω_3^*. Summarizing, for the purpose of achieving the spin-axis stabilization, our goal for control is to make partial states w_1, w_2, ω_1 and ω_2 converge to zero. When the system arrives at this state, (33), (34), (36) and (37) are reduced to

$$u_1^* = \dot{h}_1^* = h_2^*\omega_3^*, \tag{39}$$

$$u_2^* = \dot{h}_2^* = -h_1^*\omega_3^*. \tag{40}$$

From (39) and (40), it follows that the relative angular momenta of the wheels and the input control torques at convergence are sinusoidal functions.

B. Controller Design

We closely follow [8] for our controller design. Consider the following control law

$$u_1 = (I_2 - I_3)\omega_2\omega_3 + h_2\omega_3 + v_1, \tag{41}$$

$$u_2 = (I_3 - I_1)\omega_3\omega_1 - h_1\omega_3 + v_2, \tag{42}$$

where the synthetic control inputs v_1 and v_2 are defined as

$$v_1 = \kappa_1 \left[w_1 \cos(z) + w_2 \sin(z) \right] + \kappa_2 \omega_1, \tag{43}$$

$$v_2 = \kappa_1 \left[w_2 \cos(z) - w_1 \sin(z) \right] + \kappa_2 \omega_2, \tag{44}$$

with positive constant gains κ_1 and κ_2. We now show that the above control law makes the system (30)–(37) to converge to the equilibrium state discussed in Sect. IV-A:

$$w_1^* = w_2^* = \omega_1^* = \omega_2^* = 0. \tag{45}$$

Proof: Consider the following positive definite Lyapunov candidate function from [8]:

$$V = \frac{1}{2}(I_1 - J_a)\omega_1^2 + \frac{1}{2}(I_2 - J_a)\omega_2^2 + \kappa_1 \ln(1 + w_1^2 + w_2^2). \tag{46}$$

By taking time derivative of V and substituting (30), (31), (33) and (34) together with the control law (41)–(44), we obtain

$$\dot{V} = -\kappa_2(\omega_1^2 + \omega_2^2), \tag{47}$$

which is negative semi-definite. Since V is decrescent and radially unbounded, the equilibrium (45) is globally stable but it is not guaranteed to be asymptotically stable [20].

Thus, the asymptotic stability of the equilibrium state (45) is proved by LaSalle's invariance principle [20], [21]. In (47), $\dot{V} = 0$ implies that $\omega_1 = \omega_2 = 0$ and thus $\dot{\omega}_1 = \dot{\omega}_2 = 0$, provided that this corresponds to the equilibrium. By substituting this, together with (41) and (42), into (33) and (34), we obtain $v_1 = v_2 = 0$. From (43) and (44), we notice that this implies $w_1 = w_2 = 0$. Therefore, the only element in the invariance set satisfying $\dot{V} = 0$ is the equilibrium (45), and we conclude that this equilibrium is globally and asymptotically stable. ■

C. Simulations

The controller is simulated on the system consisting of a cubic rigid body and two reaction wheels attached to the body, as depicted in Fig. 2. Such a system may represent a thruster system used for hopping of tensegrity robots. In that case, the cubic rigid body would be a package of thruster system components such as compressed propellant tanks, pressure valves, thruster nozzles, etc.

In the authors' previous work [15], we have presented a tensegrity robot that can hop using a cold gas thruster. The goals of this robot are to travel over a 1 km distance on the Moon's surface and to safely deliver a 1 kg payload. The total weight of this robot is limited to 10 kg, including the payload, structural components and thruster system, in order to reduce the mission cost. These requirements were specified by NASA for our research program and are intended to facilitate low-cost surveillance missions launched as a secondary payload on a stationary lander.

For this robot, it is estimated that the cubic rigid body will have a width of 0.25 m and a total mass of 5 kg in order to carry sufficient amount of propellant required for the mission. Furthermore, we assume that the wheels are made of aluminum and each wheel has a radius of 0.077 m and thickness of 0.005 m such that its total mass is 0.25 kg.

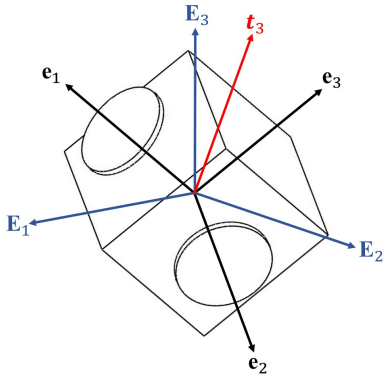

Fig. 2. A cubic rigid body with two identical axis-symmetric reaction wheels. The rotation axes of the wheels are aligned with $\mathbf{e}_1$ and $\mathbf{e}_2$.

Under these assumptions, if the body and the wheels have a uniform mass distribution, $I_1 = I_2 = 0.053$ kg m^2, $I_3 = 0.052$ kg m^2 and $J_a = 0.00037$ kg m^2.

Let us consider the case when the initial attitude of the rigid body is such that $\mathbf{e}_1 = \mathbf{E}_2$, $\mathbf{e}_2 = \mathbf{E}_3$ and $\mathbf{e}_3 = \mathbf{E}_1$. That is,

$$\mathbf{R}^0 = \begin{bmatrix} 0 & 1 & 0 \\ 0 & 0 & 1 \\ 1 & 0 & 0 \end{bmatrix}, \tag{48}$$

where the superscript ^{0} represents the initial condition. Furthermore, let the target thrust direction be given by $\mathbf{t}_3 = \frac{1}{\sqrt{2}}(\mathbf{E}_2 + \mathbf{E}_3)$, and therefore

$$\mathbf{R}_1 = \begin{bmatrix} 1 & 0 & 0 \\ 0 & \frac{1}{\sqrt{2}} & -\frac{1}{\sqrt{2}} \\ 0 & \frac{1}{\sqrt{2}} & \frac{1}{\sqrt{2}} \end{bmatrix}. \tag{49}$$

If the $\mathbf{E}_1$–$\mathbf{E}_2$ plane represents the ground surface, then $\mathbf{t}_3$ would make 45° angle with the ground, a desirable state for a parabolic hopping trajectory.

The initial attitude parameters $w^0 = w_1^0 + i w_2^0$ and z^0 can be obtained from $\mathbf{R}_3^0 \mathbf{R}_2^0 = \mathbf{R}_3(z^0)\mathbf{R}_2(w^0) = \mathbf{R}^0 \mathbf{R}_1^{\mathrm{T}}$. From (8) and (12), notice that the third row of $\mathbf{R}_3(z^0)\mathbf{R}_2(w^0)$ is

$$\left[\mathbf{R}_3^0 \mathbf{R}_2^0\right]_{(3,*)} = \begin{bmatrix} -a^0 & -b^0 & c^0 \end{bmatrix}. \tag{50}$$

Using (10),

$$w_1^0 = \frac{b^0}{1 + c^0}, \qquad w_2^0 = -\frac{a^0}{1 + c^0}. \tag{51}$$

For our example, $a^0 = -1$ and $b^0 = c^0 = 0$, which results in $w_1^0 = 0$ and $w_2^0 = 1$. The parameter z^0 is obtained from

$$\tan(z^0) = \frac{\left[\mathbf{R}_3^0 \mathbf{R}_2^0\right]_{(1,2)} - \left[\mathbf{R}_3^0 \mathbf{R}_2^0\right]_{(2,1)}}{\left[\mathbf{R}_3^0 \mathbf{R}_2^0\right]_{(1,1)} + \left[\mathbf{R}_3^0 \mathbf{R}_2^0\right]_{(2,2)}}, \tag{52}$$

which gives $z^0 = 135^\circ$ in our case.

Lastly, we assume that the initial angular velocities of the body are $\omega_1^0 = 0.8$ rad/s, $\omega_2^0 = 0.5$ rad/s and $\omega_3^0 = -0.3$ rad/s, and that the initial relative angular velocities of the wheels with respect to the primary body are zero, i.e., $h_1^0 = h_2^0 = 0$. These conditions are chosen as an example motion of the hopping tensegrity robot.

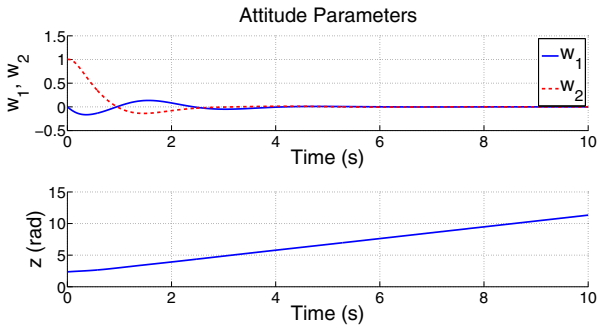

Fig. 3. Change of attitude parameters over time under control action. w_1 and w_2 converge to zero while z increases linearly, which implies that the body rotates about its spin axis at the equilibrium.

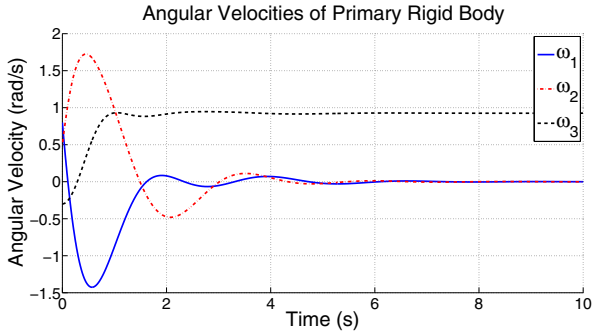

Fig. 4. Change of angular velocities over time under control action. ω_1 and ω_2 converge to zero while ω_3 converges to a nonzero constant value. This implies that the body rotates about its spin axis at the equilibrium.

The simulation results with these initial conditions and control gains of $\kappa_1 = 0.5$ and $\kappa_2 = 0.1$ are presented in Figs. 3–7. In Figs. 3 and 4, we see that the system arrives at the equilibrium (45) at around $t = 6$ s by the control action. Moreover, at this equilibrium, the body rotates about its spin axis at a constant angular speed ω_3^*. Because of this, the angle z increases linearly, but this nonzero rotation rate around the spin axis does not affect the thrust direction if the nozzle axis is aligned with the body spin axis. Figure 5 shows that the absolute angle between $\mathbf{e}_3$ and $\mathbf{t}_3$ converges to zero, meaning that they are aligned together as desired, at the equilibrium. As discussed in Sect. IV-A, the relative angular momenta of the wheels (h_1 and h_2) and the input control torques (u_1 and u_2) become sinusoidal functions of time at the equilibrium (Figs. 6 and 7). On the other hand, both synthetic control inputs v_1 and v_2 converge to zero (Fig. 7). Figure 6 shows that the total angular momentum of the system given by

$$H = \sqrt{(I_1\omega_1 + h_1)^2 + (I_2\omega_2 + h_2)^2 + (I_3\omega_3)^2}, \qquad (53)$$

is conserved because no external torques were applied to the system.

In the above simulation, although the system started with a quite large angular displacement from the target direction and nonzero angular velocities, it quickly converged to the desired equilibrium. The required input torques are small, and thus the control can be implemented with low-torque and potentially lightweight actuators. This makes the control law

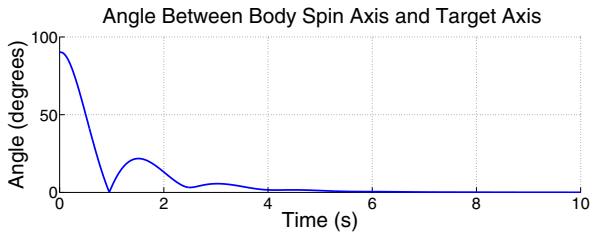

Fig. 5. Change of angle between the body spin axis $\mathbf{e}_3$ and target axis $\mathbf{t}_3$ over time. The angle converges to zero, meaning that $\mathbf{e}_3$ and $\mathbf{t}_3$ are aligned at the equilibrium.

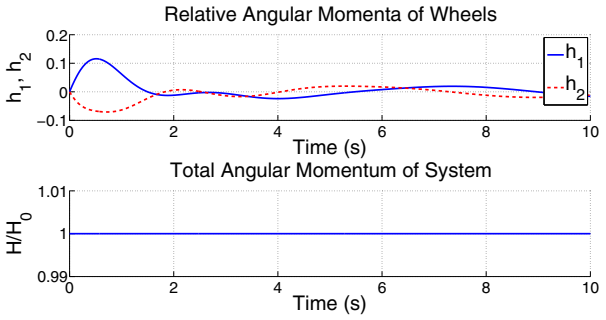

Fig. 6. Change of relative angular momenta of the wheels with respect to the primary body over time. At the equilibrium, both h_1 and h_2 become sinusoidal functions of time. The total angular momentum of the system, H, is conserved.

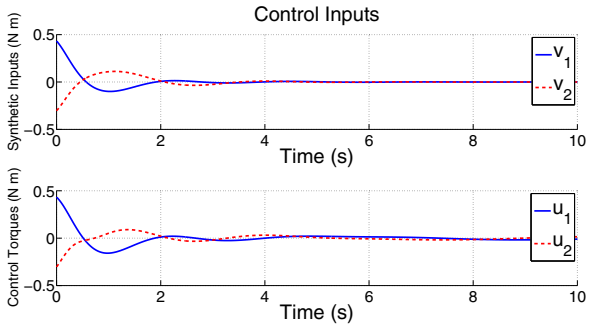

Fig. 7. Change of control inputs over time. Both synthetic control inputs v_1 and v_2 converge to zero. The input control torques u_1 and u_2 become sinusoidal functions of time at the equilibrium.

particularly promising for hopping tensegrity robots where the total weight of the system is a critical factor.

An interesting case arises when both the body and the wheels are not rotating initially, that is, when the total angular momentum H of the system is initially zero. Because the total angular momentum is conserved, it should remain at zero when the equilibrium state is reached. As a result, $h_1^* = h_2^* = \omega_3^* = 0$, which implies that the body and the wheels become stationary at the equilibrium without spinning. This observation was also discussed in [2]. For a tensegrity hopper, this could be the case of reorienting the thruster nozzle in mid-air, assuming that the hopper was launched in such a way that its angular velocities are zero and the reaction wheels do not rotate. We present simulation of this case in the next.

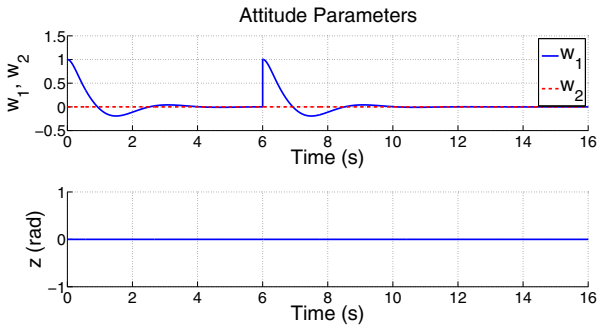

Fig. 8. Change of attitude parameters over time under control action for the singular case. w_1 first converges to zero at around $t = 6$ and then again to zero at around $t = 12$. The first convergence corresponds to the stabilization of the body spin axis $\mathbf{e}_3$ about $\mathbf{t}'_3 = \mathbf{E}_2$, and the next one about $\mathbf{t}_3 = -\mathbf{E}_3$. Unlike the first example, w_2 and z remain zero throughout. Because the initial angular momentum of the whole system is zero, the body and the wheels do not rotate at the equilibrium.

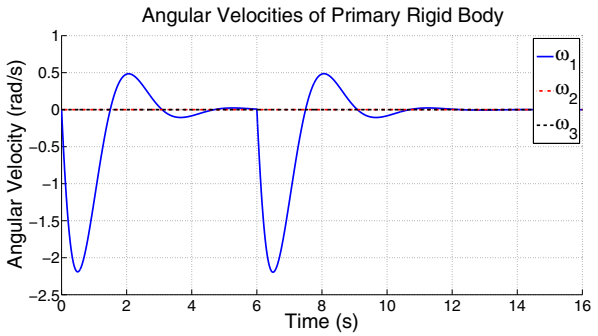

Fig. 9. Change of angular velocities over time under control action for the singular case. ω_1 first converges to zero at around $t = 6$ and then again to zero at around $t = 12$. The first convergence corresponds to the stabilization of the body spin axis $\mathbf{e}_3$ about $\mathbf{t}'_3 = \mathbf{E}_2$, and the next one about $\mathbf{t}_3 = -\mathbf{E}_3$. ω_2 and ω_3 remain zero throughout. Because the initial angular momentum of the whole system is zero, the body and the wheels do not rotate at the equilibrium.

Figures 8–12 show another simulation results, with the same physical parameters and control gains as in the previous simulation, where the singularity discussed in Sect. II-C arises. That is, the target axis is exactly at the opposite direction of the current body spin axis. Specifically, in this simulation, we assumed the principal axes of the primary body are initially aligned with the inertial axes ($\mathbf{e}_j = \mathbf{E}_j$, $j = 1, 2, 3$) and our target frame is given by $\mathbf{t}_1 = \mathbf{E}_1$, $\mathbf{t}_2 = -\mathbf{E}_2$ and $\mathbf{t}_3 = -\mathbf{E}_3$. This target frame is easily achieved by rotating the inertial frame by 180° about $\mathbf{E}_1$. However, our kinematics description results in $a^0 = b^0 = 0$ and $c^0 = -1$ and thus the target configuration is singular. To overcome this singularity, we take a two-step process as suggested in Sect. II-C: 1) We first stabilize $\mathbf{e}_3$ about $\mathbf{t}'_3 = \mathbf{E}_2$ by rotating the body -90° about $\mathbf{E}_1$, and then 2) stabilize $\mathbf{e}_3 = \mathbf{t}'_3$ about $\mathbf{t}_3 = -\mathbf{E}_3$ by further rotating the body -90° about $\mathbf{E}_1$. Recall that we further assumed the initial angular velocities and angular momenta of the system are equal to zero in this simulation. As a consequence, the total angular momentum of the system remains zero (Fig. 11), and the angular velocities and attitude parameters converge to zero at the equilibrium (Figs. 8 and 9).

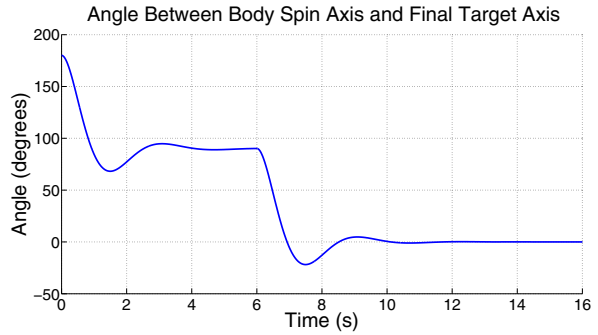

Fig. 10. Change of angle between the body spin axis $\mathbf{e}_3$ and the final target axis $\mathbf{t}_3 = -\mathbf{E}_3$ over time for the singular case. The angle converges to zero at around $t = 12$, meaning that $\mathbf{e}_3$ and $\mathbf{t}_3$ are aligned at the equilibrium.

V. Conclusion and Future Research

We presented a control law achieving the spin-axis stabilization of a rigid body about an arbitrary direction using two reaction wheels. Specifically, our control law successfully achieved two goals: 1) it oriented the spin axis of the body to an arbitrary direction, and 2) it made the body rotate about the spin axis only, if the angular momentum of the system is not zero. The control law was developed using a feedback linearization technique and it was shown that the control is globally and asymptotically stable about the equilibrium (45) by using Lyapunov's direct method in conjunction with LaSalle's invariance principle. In addition, the new set of differential kinematic equations that are based on the (z, w)-parameterization is derived. The new formulation explicitly considers the arbitrary target direction about which the spin

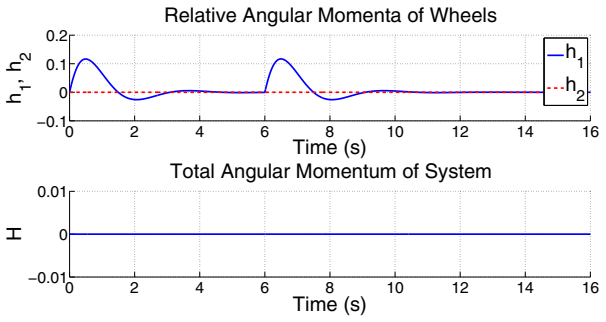

Fig. 11. Change of relative angular momenta of the wheels with respect to the primary body over time for the singular case. h_1 first converges to zero at around $t = 6$ and then again to zero at around $t = 12$. The first convergence corresponds to the stabilization of the body spin axis $\mathbf{e}_3$ about $\mathbf{t}'_3 = \mathbf{E}_2$, and the next one about $\mathbf{t}_3 = -\mathbf{E}_3$. h_2 remains zero throughout. The total angular momentum of the system, H, is conserved and is equal to zero.

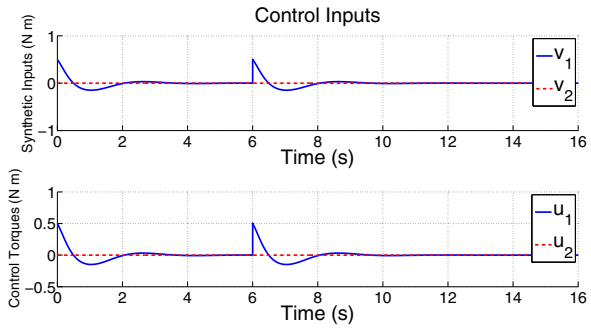

Fig. 12. Change of control inputs over time for the singular case. Both v_1 and u_1 first converge to zero at around $t = 6$ and then again to zero at around $t = 12$. The first convergence corresponds to the stabilization of the body spin axis $\mathbf{e}_3$ about $\mathbf{t}'_3 = \mathbf{E}_2$, and the next one about $\mathbf{t}_3 = -\mathbf{E}_3$. v_2 and u_2 remain zero throughout.

axis of the body is stabilized, and describes the attitude of the body with respect to the target orientation.

We also demonstrated the stabilizing behavior of the controller by simulating it on a thruster system of hopping tensegrity robots. It was shown that our control law can quickly orient the thruster nozzle to a desired target direction using lightweight wheels and small control torques that can potentially be provided by lightweight actuators. We further simulated the strategy to overcome the singularity that arises from the stereographic projection.

In this work, it was assumed that the perfect knowledge of the states is provided when developing and simulating the controller. In practice, however, this information may not be available and there may exist signal noises, model uncertainties and external disturbances that challenge the controller. Our future research will focus on the development of a robust controller that performs well even under these unfavorable conditions.

ACKNOWLEDGMENT

The authors gratefully acknowledge partial funding for this research through NASA Early Stage Innovations grant NNX15AD74G, NASA Innovative Advanced Concepts Program and UARC STI Graduate Student Summer Internship. We also thank for the valuable feedback from Andrew P. Sabelhaus, Brian Cera, Adrian K. Agogino and BEST Lab members from UC Berkeley.

REFERENCES

[1] P. E. Crouch, "Spacecraft attitude control and stabilization: Applications of geometric control theory to rigid body models," *Automatic Control, IEEE Transactions on*, vol. 29, no. 4, pp. 321–331, 1984.

[2] H. Krishnan, H. McClamroch, and M. Reyhan, "On the attitude stabilization of a rigid spacecraft using two control torques," in *American Control Conference, 1992*. IEEE, 1992, pp. 1990–1995.

[3] C. I. Byrnes and A. Isidori, "On the attitude stabilization of rigid spacecraft," *Automatica*, vol. 27, no. 1, pp. 87–95, 1991.

[4] P. Morin and C. Samson, "Time-varying exponential stabilization of a rigid spacecraft with two control torques," *Automatic Control, IEEE Transactions on*, vol. 42, no. 4, pp. 528–534, 1997.

[5] T. Urakubo, K. Tsuchiya, and K. Tsujita, "Attitude control of a spacecraft with two reaction wheels," *Journal of Vibration and Control*, vol. 10, no. 9, pp. 1291–1311, 2004.

[6] Y. Katsuyama, K. Sekiguchi, and M. Sampei, "Spacecraft attitude control by 2 wheels with initial angular momentum," in *SICE Annual Conference (SICE), 2013 Proceedings of*. IEEE, 2013, pp. 1890–1895.

[7] Y. Katsuyama, T. Ibuki, K. Sekiguchi, and M. Sampei, "Attitude controllability analysis of an underactuated satellite with two reaction wheels and its control," in *Proceedings of 2015 IEEE 54th Annual Conference on Decision and Control (CDC)*. IEEE, 2015, pp. 3421–3426.

[8] S. Kim and Y. Kim, "Spin-axis stabilization of a rigid spacecraft using two reaction wheels," *Journal of Guidance, Control, and Dynamics*, vol. 24, no. 5, pp. 1046–1049, 2001.

[9] P. Tsiotras and J. M. Longuski, "Spin-axis stabilization of symmetric spacecraft with two control torques," *Systems & Control Letters*, vol. 23, no. 6, pp. 395–402, 1994.

[10] R. B. Fuller, "Tensile-integrity structures," Patent US 3 063 521A, Nov. 13, 1962.

[11] A. K. Agogino, V. SunSpiral, and D. Atkinson, "Super Ball Bot – Structures for planetary landing and exploration," *NASA Innovative Advanced Concepts (NIAC) Program, Phase 1, Final Report*, Jul. 2013.

[12] V. SunSpiral, A. K. Agogino, and D. Atkinson, "Super Ball Bot – Structures for planetary landing and exploration," *NASA Innovative Advanced Concepts (NIAC) Program, Phase 2, Final Report*, Sep. 2015.

[13] V. SunSpiral, G. Gorospe, J. Bruce, A. Iscen, G. Korbel, S. Milam, A. K. Agogino, and D. Atkinson, "Tensegrity based probes for planetary exploration: Entry, descent and landing (EDL) and surface mobility analysis," *International Journal of Planetary Probes*, 2013.

[14] K. Kim, A. K. Agogino, D. Moon, L. Taneja, A. Toghyan, B. Dehghani, V. SunSpiral, and A. M. Agogino, "Rapid prototyping design and control of tensegrity soft robot for locomotion," in *Proceedings of 2014 IEEE International Conference on Robotics and Biomimetics (ROBIO2014)*, Bali, Indonesia, Dec. 2014, *Finalist Best Student Paper*.

[15] K. Kim, L.-H. Chen, B. Cera, M. Daly, E. Zhu, J. Despois, A. K. Agogino, V. SunSpiral, and A. M. Agogino, "Hopping and rolling locomotion with spherical tensegrity robots," in *Proceedings of 2016 IEEE/RSJ International Conference on Intelligent Robots and Systems (IROS 2016)*, Daejeon, South Korea, Oct. 2016.

[16] A. P. Sabelhaus, J. Bruce, K. Caluwaerts, Y. Chen, D. Lu, Y. Liu, A. K. Agogino, V. SunSpiral, and A. M. Agogino, "Hardware design and testing of SUPERball, a modular tensegrity robot," in *Proceedings of The 6th World Conference of the International Association for Structural Control and Monitoring (6WCSCM)*, Barcelona, Spain, Jul. 2014.

[17] J. Bruce, A. Sabelhaus, Y. Chen, D. Lu, K. Morse, S. Milam, K. Caluwaerts, A. M. Agogino, and V. SunSpiral, "SUPERball: Exploring tensegrities for planetary probes," in *Proceedings of 12th International Symposium on Artificial Intelligence, Robotics and Automation in Space (i-SAIRAS 2014)*, Montreal, Canada, Jun. 2014.

[18] P. Tsiotras and J. M. Longuski, "A new parameterization of the attitude kinematics," *Journal of the Astronautical Sciences*, vol. 43, no. 3, pp. 243–262, 1995.

[19] J. L. Junkins and J. D. Turner, *Optimal spacecraft rotational maneuvers*. Elsevier, 1986.

[20] H. K. Khalil and J. Grizzle, *Nonlinear systems*. Prentice hall New Jersey, 1996, vol. 3.

[21] J. LaSalle, "Stability theory for ordinary differential equations," *Journal of Differential Equations*, vol. 4, no. 1, pp. 57–65, 1968.